Electronic Supplementary Material (ESI) for Nanoscale.

Supporting Information

Fuzzy copper-based multi-functional composite particles serving simultaneous catalytic and signal-enhancing roles

Xiangming Li, Yingmo Hu[*], Qi An[*], Xinglong Luan, Qian Zhang, Yihe Zhang[*]

Beijing Key Laboratory of Materials Utilization of Nonmetallic Minerals and Solid Wastes, National Laboratory of Mineral Materials, School of Materials Science and Technology, China University of Geosciences, Beijing, 100083, China.

1. Experimental details:

Measurement of photothermal performance

The rGO/(PEI/PAA)$_3$/PEI-CuNPs dispersion (0.25 mg/mL) was irradiated for 15 min using an infrared lasers (940 nm, power density 1.0 W/cm^2). The temperature of the solution was measured each minute. The rGO/(PEI/PAA)$_3$/PEI dispersions (0.25 mg/mL) and the copper nanoparticles (CuNPs, 0.25 mg/mL) synthesized using sodium borohydride as the reducing reagent[1] were used as controls.

Fabrication of rGO/(PEI/PAA)$_n$/PEI thin film on the quartz plates

The quartz plates were treated by immersion in H_2SO_4/H_2O_2 (7:3) solution for 24 h and then dried by nitrogen flow after washing with a copious amount of deionized water. The prepared quartz plates were immersed in the rGO/PEI dispersion (0.25 mg/mL) for 10 min, followed by washing with a copious amount of deionized water and dried by nitrogen flow. Subsequently, the plates were immersed in PAA solution (5 mg/mL, pH 3.8) for 10 min. Then the quartz plates were washed with a copious amount of deionized water and dried by nitrogen flow. The rGO/PEI dispersion was taken place by PEI solution (5 mg/mL, pH 9.0) in the following LbL assembly process. The rGO/(PEI/PAA)$_n$/PEI thin film on the quartz plates were obtained in a similar method by repeating the above-mentioned steps. The LbL growth processes were monitored by UV−vis spectroscopy.

Permeation measurement of rGO/(PEI/PAA)$_n$/PEI thin film on the quartz plates

The quartz plates with different layers of the thin film were immersed into the saturated 4-amionphenol solution. After 1 h, the quartz plates were washed briefly with a copious amount of deionized water and dried by nitrogen flow. The permeation performance was monitored by UV−vis spectroscopy.

2. FTIR of rGO/(PEI/PAA)$_3$/PEI-CuNPs complex

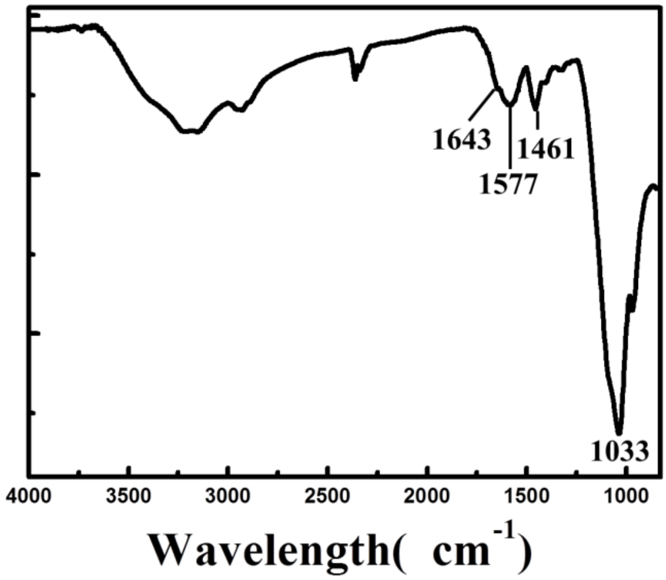

Figure S1. FTIR spectra of the rGO/(PEI/PAA)$_3$/PEI-CuNPs complex.

3. Elemental mapping of the rGO/(PEI/PAA)$_3$/PEI-CuNPs complex

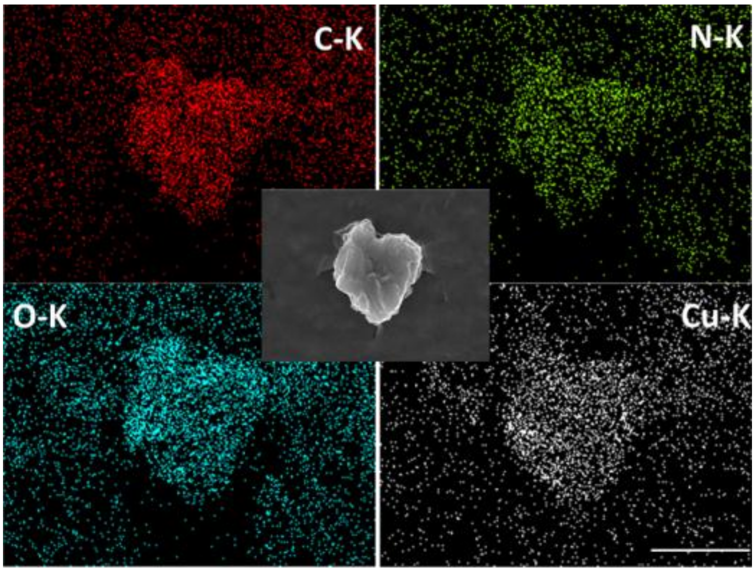

Figure S2. Elemental mapping of rGO/(PEI/PAA)$_3$/PEI-CuNPs complex. The scale bars in the images corresponded to 10 μm.

4. Color change before and after the catalytic conversion of 4-NP to 4-AP.

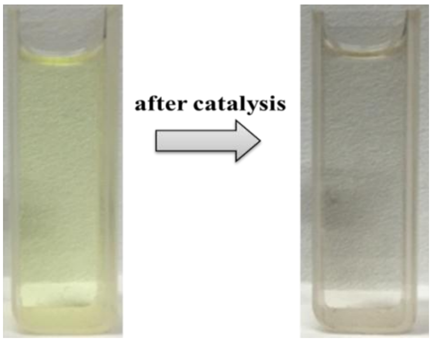

Figure S3. Optical photo of the change of the color of the reaction solution.

5. CuNPs prepared using conventional method.

The average particle size of the CuNPs was about 400 nm which was measured by Dynamic Light Scattering (DLS, data not shown). TEM image of CuNPs are shown in Figure S4b, also indicating the size of the CuNPs of 400 nm.

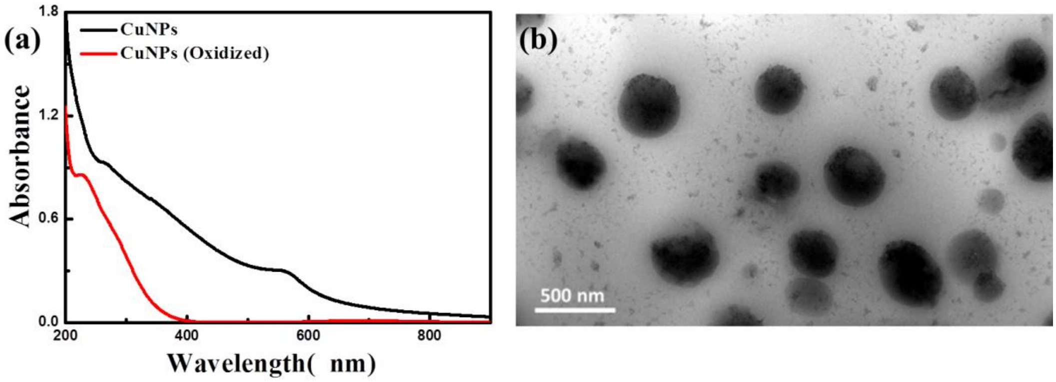

Figure S4. (a) UV-vis spectra of the CuNPs (black) synthesized using sodium borohydride as the reducing reagent and the CuNPs (red) kept overnight in ambient conditions. The spectra indicated that upon keeping overnight, the CuNPs were partially oxidized. (b) TEM image of (partially oxidized) CuNPs.

6. Catalytic conversion of 4-NP to 4-AP: controls experiments, K_{app} values, and comparisons with previously reported noble metal-graphene catalysts.

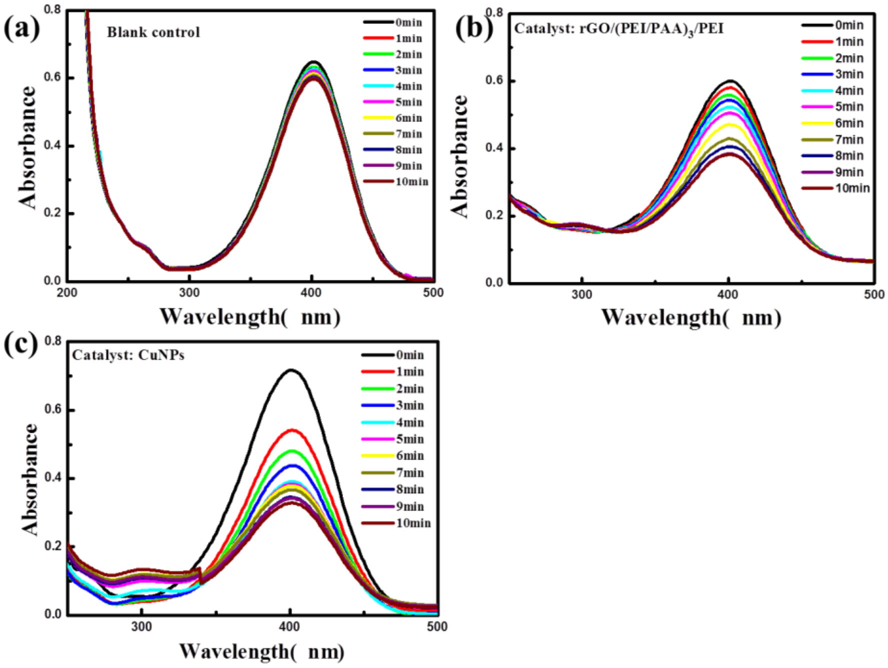

Figure S5. UV-vis spectra of process of the catalytic reaction (a) blank control, (b) with rGO/(PEI/PAA)$_3$/PEI and (c) with CuNPs synthesized using hydrazine hydrate as the reducing agent.

Table S1. The comparison of catalytic performance of rGO/(PEI/PAA)$_3$/PEI-CuNPs.

Samples	Mass (mg)	K_{app} (min^{-1})	R^2
rGO/(PEI/PAA)$_3$/PEI	0.025	0.0404	0.9735
rGO/(PEI/PAA)$_3$/PEI-CuNPs	0.025	0.2290	0.9831
CuNPs	0.028	0.1059	0.8768

Table S2. The comparison of catalytic performance of rGO/(PEI/PAA)$_3$/PEI-CuNPs complex and previously reported noble metal-graphene catalysts.

Catalyst	**K_{app} (min^{-1})**	**Catalyst conc. (mg/mL)**	**4-NP conc. (mM)**	**Reference**
rGO/(PEI/PAA)$_3$/PEI-CuNPs	0.2290	6.25×10^{-3}	3.75×10^{-2}	This work
Ag/CeO$_2$ graphene oxide	0.0388	1.27×10^{-2}	7.37×10^{-2}	2
Au/graphene oxide	0.1880	———	———	3
CuNPs/PAA	0.0852	———	———	4
Ni$_{25}$Co$_{75}$/RGO	0.0960	5.77×10^{-2}	9.62×10^{-2}	5

7. Photothermal conversion of the rGO/(PEI/PAA)$_3$/PEI-CuNPs.

Both copper/copper oxide particles and rGO are photothermal agencies.[6-7] Here we show that the composite particles present superior photothermal performance than either copper/copper oxide particles or rGO (Figure S6). Under the infrared radiation, the temperature of the rGO/(PEI/PAA)$_3$/PEI-CuNPs dispersion increased the most rapidly from 31.4 to 38.2 ℃ while the temperature of the CuNPs dispersion reached only 34.2 ℃, and the rGO/(PEI/PAA)$_3$/PEI dispersion 36.4 ℃.

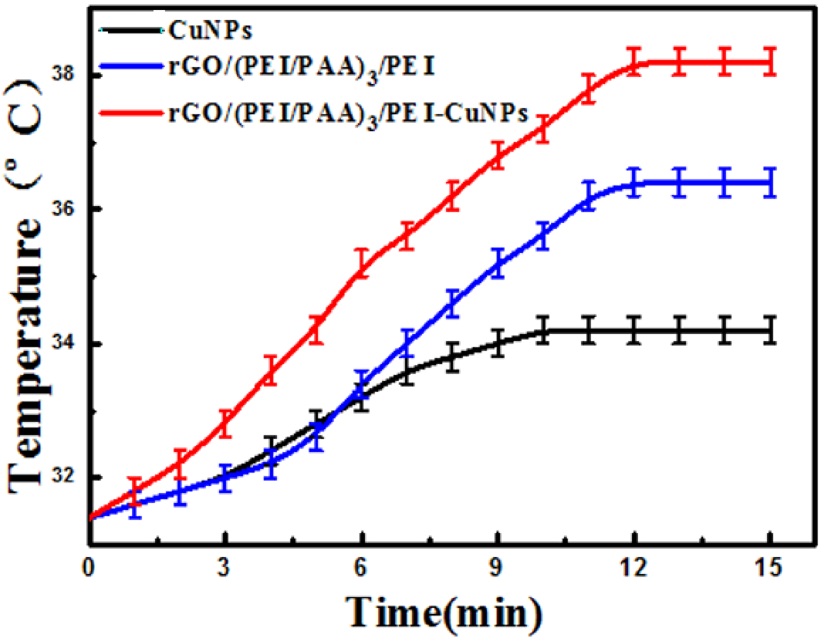

Figure S6. Photothermal performance of CuNPs prepared using sodium borohydride as the reducing and protecting agents, rGO/(PEI/PAA)$_3$/PEI complex and rGO/(PEI/PAA)$_3$/PEI-CuNPs complex.

8. Raman spectra around rGO/(PEI/PAA)$_3$/PEI-CuNPs as substrates.

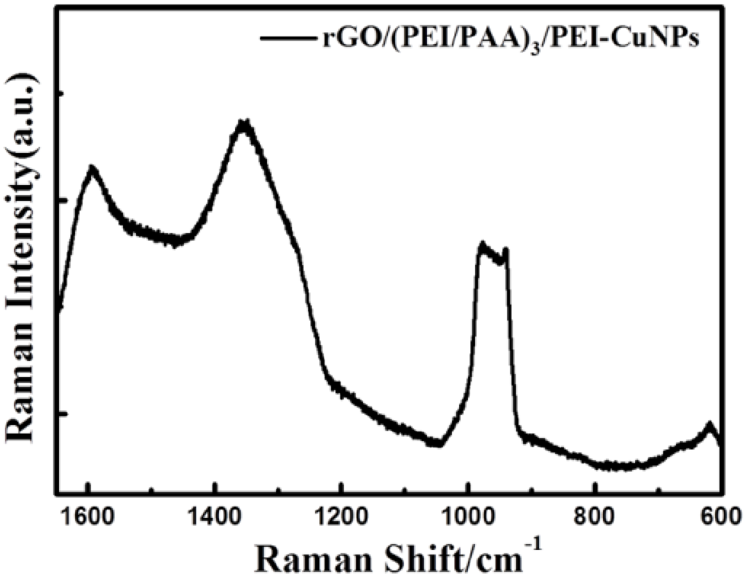

Figure S7. SERS of rGO/(PEI/PAA)$_3$/PEI-CuNPs complex.

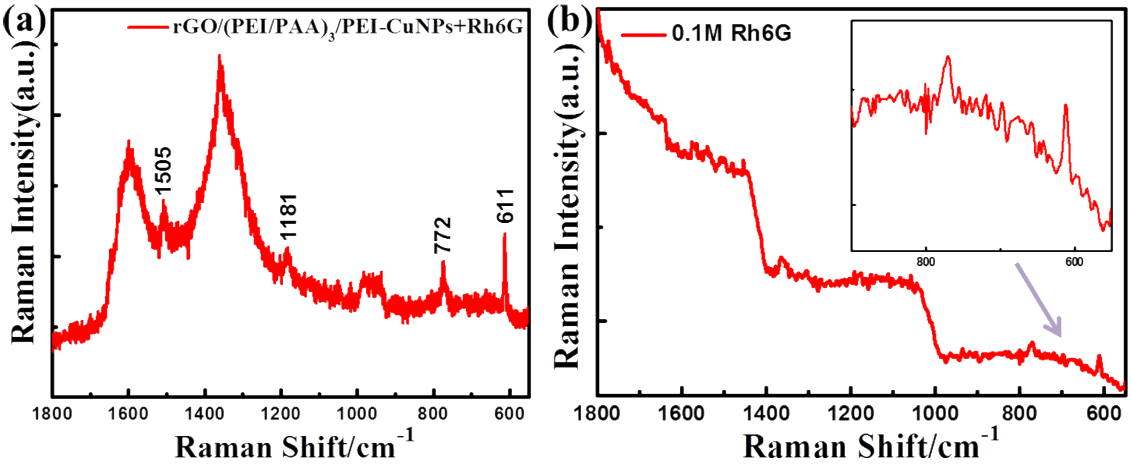

Figure S8. (a) SERS of Rh6G on the substrate of rGO/(PEI/PAA)$_3$/PEI-CuNPs composite particles. (b) Regular Raman spectra of the Rh6G solution (0.1 M).

9. The penetration nature of the polyelectrolyte multilayers to small molecules.

In order to demonstrate that the rGO/(PEI/PAA)$_n$/PEI multilayers were penetrable to small molecules and were able to hold these molecules in equilibrium with those in solution, we designed illustrative experiments on planar substrates (Figure S9a). Multilayers of rGO/(PEI/PAA)$_3$/PEI were built on quartz substrates, monitored by UV−visible spectra. The absorbance increased gradually with the growth of the number of bilayers, indicating the successful assembly of the multilayers, as shown in Figure S9b. Upon immersion into a solution of 4-AP, the characteristic absorbance of 4-AP at around 310 nm increased in accordance with the increase of the number of bilayers，indicating that the film was penetrable to 4-AP and was able to hold the small molecules in bulk film in equilibrium with the molecules in solution (Figure S9c).

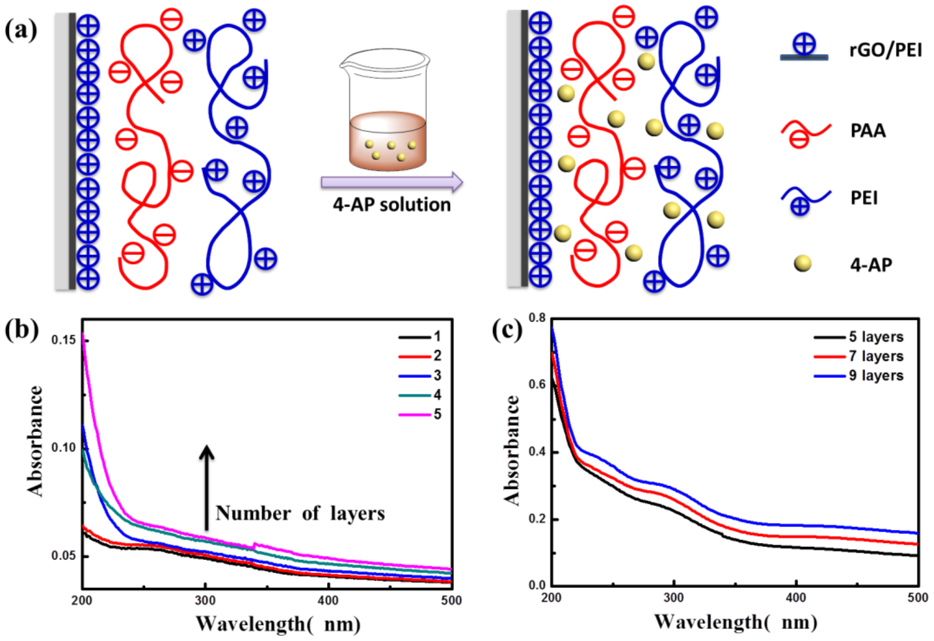

Figure S9. (a) Illustrative experimental setup for thepenetration nature of the polyelectrolyte multilayers to 4-AP,UV-vis spectra of (b) process of therGO/(PEI/PAA)$_n$/PEI thin film on the quartz plates and (c) the permeability of 4-AP with different layers.

References

1. Q. M. Liu, D. B. Zhou, Y. Yamamoto, R. Ichino and M. Okido, *Tram. Nonferrous Met. Soc. China*, 2012, **22**, 117-123.

2. Z. Ji, X. Shen, J. Yang, G. Zhu and K. Chen, *Appl. Catal. B*, 2014, **144**, 454-461.

3. Y. Zhang, S. Liu, W. Lu, W. Lei, J. Tian and X. Sun, *Catal.sci.technol*, 2011, **1**, 1142-1144.

4. R. Kaur, C. Giordano, M. Gradzielski and S. K. Mehta, *Chem. Asian J.*, 2014, **9**, 189-198.

5. B. Song, X. Shen, G. Zhu, M. Li, H. Xi and K. Chen, *ACS Appl. Mater. Interfaces*, 2012, **4**, 2378-2386.

6. K. Nie, Q. An, S. Tao, Z. Zhang, X. Luan, Q. Zhang and Y. Zhang, *RSC Adv*., 2015, **5**, 57389-57394.

7. C. A. Tao, X. Zou, Z. Hu, H. Liu and J. Wang, *Polym. Compos.*, 2014, DOI: 10.1002/pc.23303.